

## Auralization in space and in rooms of arbitrary $D$ dimensions

Felipe Orduña-Bustamante

Centro de Ciencias Aplicadas y Desarrollo Tecnológico,  
 Universidad Nacional Autónoma de México,  
 Circuito Exterior S/N, Ciudad Universitaria,  
 Del. Coyoacán, C.P. 04510, México D.F., MÉXICO.  
 felipe.orduna@ccadet.unam.mx

### ABSTRACT

Signal processing and computing procedures are presented to imprint, into any given audio signal (preferably obtained from a dry anechoic recording), the temporal and spectral characteristics of radiation of simple sources in free field, and in reverberant rectangular rooms, that could virtually be obtained in space of any spatial dimensions  $D \geq 1$ . These techniques are based on mathematically exact solutions of the conventional acoustic field equations, usually expressed and solved for space of three dimensions or less, but generalized formally to describe the analogue to sound waves in space of higher dimensions. Processing as presented here is monaural, but the mathematical tools exist to imprint a hyper-angular dependence in higher dimensions, and to map that into conventional binaural presentations. Working computer implementations, and sound samples are presented. The foreseen applications include: sonic art, virtual reality, extended reality, videogames, computer games, and others.

### 1. INTRODUCTION

The subject of high-dimensional wave equations has been extensively developed in Applied Quantum Mechanics, in dealing with quantum systems with many bodies [1–4]. Schrodinger’s equation for a system of  $N$  bodies, involves a wave equation in a coordinate or momentum space of dimension  $D = 3N - 1$ , after removing the motion of the center of mass. Most of that analysis separates a radial part of the solution, from a hyper-angular part [5–7]. This article deals with the adaptation of radial part solutions, to solve the corresponding equations of acoustics for a radial sound pressure field in space of arbitrary  $D$  dimensions. Radiation of simple acoustic sources are then combined with the source image method [8], in order to simulate a reverberant sound field in a room of  $D$  dimensions. Further work on this subject will probably involve dealing with the hyper-angular part of the higher-dimensional wave equation [9, 10], and devising some sort of mapping the resulting audio into conventional binaural sound presentations.

Copyright: © 2017 Felipe Orduña-Bustamante et al. This is an open-access article distributed under the terms of the [Creative Commons Attribution 3.0 Unported License](https://creativecommons.org/licenses/by/3.0/), which permits unrestricted use, distribution, and reproduction in any medium, provided the original author and source are credited.

Formulations using finite-difference time-domain FDTD methods have also been developed by others [11, 12].

### 2. RADIAL SOUND WAVES IN $D$ DIMENSIONS

The acoustic field equations for the sound pressure  $p(\mathbf{x}, \omega)$ , and particle fluid velocity  $\mathbf{u}(\mathbf{x}, \omega)$  in the frequency domain  $\omega$ , assuming a complex harmonic time dependence of the form  $e^{+j\omega t}$ , are as follows:

$$\text{grad } p(\mathbf{x}, \omega) = -jkZ_0\mathbf{u}(\mathbf{x}, \omega), \quad (1)$$

$$\text{div } \mathbf{u}(\mathbf{x}, \omega) = -jkZ_0^{-1}p(\mathbf{x}, \omega); \quad (2)$$

where  $k = \omega/c_0$  is the acoustic wavenumber,  $Z_0 = \rho_0 c_0$  is the characteristic acoustic impedance,  $c_0$  is the speed of sound, and  $\rho_0$  is mass density of the propagation medium. These can be written for a radial field in  $D$  dimensions in the form:

$$\frac{\partial p}{\partial r} = -jkZ_0 u_r(r), \quad (3)$$

$$\frac{1}{r^{D-1}} \frac{\partial}{\partial r} (r^{D-1} u_r) = -jkZ_0^{-1} p(r). \quad (4)$$

These remain similar to its usual form, as in cylindrical, or spherical coordinates in  $D = 2, 3$ .

The radial part of the in-homogeneous Helmholtz equation can be written as follows:

$$\nabla^2 p(r) + k^2 p(r) = -q(r), \quad (5)$$

$$\frac{\partial^2 p}{\partial r^2} + (D-1) \frac{1}{r} \frac{\partial p}{\partial r} + k^2 p(r) = -q(r), \quad (6)$$

$$\frac{1}{r^{D-1}} \frac{\partial}{\partial r} \left( r^{D-1} \frac{\partial p}{\partial r} \right) + k^2 p(r) = -q(r). \quad (7)$$

The substitution  $p(r) = \phi(kr)/(kr)^{D/2-1}$ , turns this into Bessel’s equation of order  $\nu = D/2 - 1$ , the order  $\nu$  being zero, or a positive integer, when the space dimension  $D$  is even, and half-integer when  $D$  is odd. Solutions for  $\phi(kr)$ , correspond to Hankel functions of order  $\nu$ , in terms of which, outgoing radial waves for the sound pressure, when the source term is a spatial Dirac point distribution  $q(r) = \delta(r)$ , can be written as follows:

$$p(r, \omega) = \frac{\mathcal{A} H_\nu^{(2)}(kr)}{(kr)^{D/2-1}}, \quad (8)$$

$$\approx \frac{\sqrt{2/\pi} \mathcal{A} e^{-j[kr - (D-1)\pi/4]}}{(kr)^{(D-1)/2}}, \quad kr \gg 1; \quad (9)$$

where  $\mathcal{A}$  is the complex amplitude of the sound pressure, with corresponding expressions for the particle velocity. Additional terms can also include incoming waves.

### 2.1 The simple monopole source in $D$ dimensions

The radiation transfer function  $\mathcal{M}_D(r, \omega)$  of a simple monopole source can be defined as the ratio between the outgoing sound pressure wave amplitude in the far field, to the volume velocity in the near field,  $Q_0(\omega)$ , with  $q(r) = j\omega\rho_0 \delta(r)$ , which in  $D$  dimensions works out as follows:

$$\mathcal{M}_D(r, \omega) = (Z_0/2) \left( \frac{jk}{2\pi r} \right)^{(D-1)/2} e^{-jkr}. \quad (10)$$

Calculation of the inverse Fourier transform of  $p(r, \omega) = \mathcal{M}_D(\omega)Q_0(\omega)$ , involves considering the time delay operator:  $e^{-j\omega r/c_0} \longleftrightarrow \delta(t - r/c_0)$ , the derivative operator:  $(j\omega)^\nu \longleftrightarrow d^\nu/dt^\nu$ , and for  $D$  even, the half-integration operator:  $(j\omega)^{-1/2} \longleftrightarrow (\pi t)^{-1/2}$ , implied by the required half-integer (fractional) derivatives. The corresponding expressions in the time domain, are as follows:

$$p(r, t) = \frac{(Z_0/2)}{(1/2\pi r c_0)^{(D-1)/2}} \times \quad (11)$$

$$Q_0^{[(D-1)/2]}(t - r/c_0), \quad D \text{ odd},$$

$$= \frac{(Z_0/2)}{(1/2\pi r c_0)^{(D-1)/2}} \times \quad (12)$$

$$\int_0^\infty \frac{Q_0^{[D/2]}(t - r/c_0 - \tau)}{(\pi\tau)^{1/2}} d\tau, \quad D \text{ even};$$

where Fourier transform pairs are indicated by their arguments:  $p(r, t) \longleftrightarrow p(r, \omega)$ ,  $Q_0(r, t) \longleftrightarrow Q_0(r, \omega)$ , and with time derivatives indicated by  $Q_0^{[\nu]}(t) = d^\nu Q_0(t)/dt^\nu$ . The first expression, Eq. (11), is formally valid also for  $D$  even, but in that case, a fractional derivative is implied, which should be understood as in the second expression, Eq. (12). Figure 1 shows sound pressure pulses radiated identically and simultaneously by two monopole sources at duplicate distances in space of dimensions  $D = 1$  to 6.

## 3. RECTANGULAR ROOMS IN $D$ DIMENSIONS

### 3.1 The image method in one dimension, $D = 1$

In a one dimensional cavity with rigid ends, the characteristic functions  $\phi_m(x)$ , and characteristic values  $k_m$ , satisfying the Helmholtz equation, and the rigid boundary conditions, are as follows:

$$\frac{\partial^2 \phi_m}{\partial x^2} \phi_m + k_m^2 \phi_m(x) = 0, \quad (13)$$

$$\partial \phi_m / \partial x = 0, \quad x = 0, L, \quad (14)$$

$$\phi_m(x) = (2/L)^{1/2} \cos k_m x, \quad (15)$$

$$k_m = m\pi/L, \quad (16)$$

$$\int_0^L dx \phi_m(x) \phi_n(x) = \delta_{mn}. \quad (17)$$

The fundamental solution, or Green's function,  $G(x, y)$ , satisfies the in-homogeneous Helmholtz equation with a

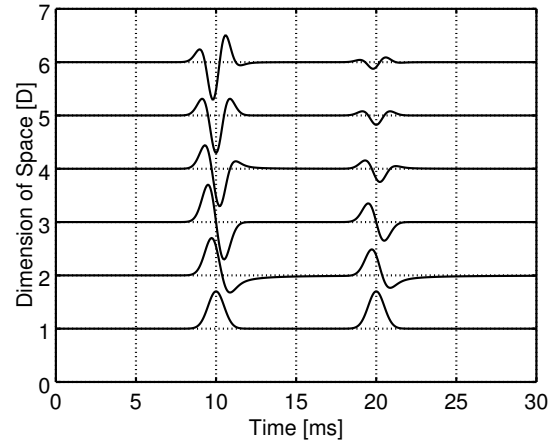


Figure 1. Sound pressure pulses radiated identically and simultaneously by two monopole sources at duplicate distances in space of dimensions  $D = 1$  to 6. Absolute peak amplitudes are normalized to 0.7 vertical units.

concentrated point source:

$$\frac{\partial^2 G}{\partial x^2} + k^2 G(x, y) = -\delta(x - y), \quad (18)$$

$$\frac{\partial G}{\partial x} = 0, \quad x = 0, L. \quad (19)$$

The fundamental solution can be expressed in terms of the characteristics functions, as follows:

$$G(x, y) = \sum_m \frac{\phi_m(x) \phi_m(y)}{k_m^2 - k^2}, \quad (20)$$

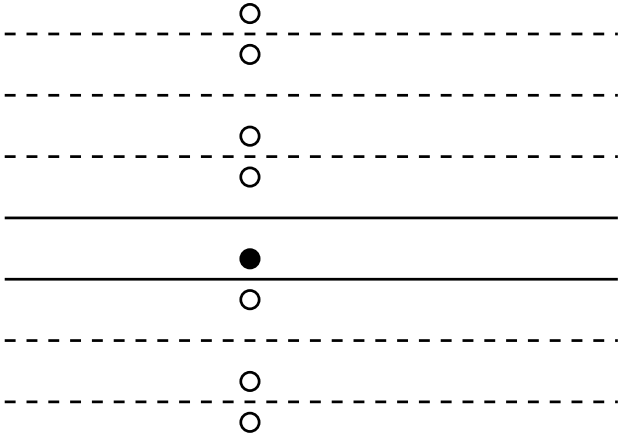
$$G(x, y) = \left( \frac{2}{L} \right) \sum_m \frac{\cos k_m x \cos k_m y}{k_m^2 - k^2}. \quad (21)$$

This representation can be transformed into the following, in terms of image sources driven at unit volume velocity,  $p(x, y) = jkZ_0 G(x, y)$ , or unit particle velocity in  $D = 1$ :

$$p(x, y) = \left( \frac{Z_0}{2} \right) \sum_{n=-\infty}^{+\infty} e^{-jk|x-y_n^+|} + e^{-jk|x-y_n^-|}, \quad (22)$$

$$= \sum_{n=-\infty}^{+\infty} \mathcal{M}_{D=1}(|x - y_n^+|, \omega) + \mathcal{M}_{D=1}(|x - y_n^-|, \omega). \quad (23)$$

This is the superposition of simple sound sources (monopoles) in two different regularly spaced, infinite arrays of image source locations:  $y_n^+ = 2Ln + y$ ,  $y_n^- = 2Ln - y$ , for all possible integer values of  $n$ . In order to take into account sound absorption at the walls, additional factors can also be included in integer powers of the corresponding reflection coefficients, depending on the number of wall reflections that each image source implies.


 Figure 2. Distribution of image sources in  $D = 1$ .

### 3.2 The image method in $D$ dimensions

The image method can be extended in a very straightforward fashion to arbitrary dimension  $D$ , as follows:

$$p(\mathbf{x}, \mathbf{y}) = \sum_{\mathbf{n}=-\infty}^{+\infty} \mathcal{M}_{D_s}(|\mathbf{x} - \mathbf{y}_{\mathbf{n}}^+|, \omega) + \mathcal{M}_{D_s}(|\mathbf{x} - \mathbf{y}_{\mathbf{n}}^-|, \omega), \quad (24)$$

$$\mathbf{x} = (x_1, x_2, x_3, \dots, x_D), \quad (25)$$

$$\mathbf{y} = (y_1, y_2, y_3, \dots, y_D), \quad (26)$$

$$\mathbf{n} = (n_1, n_2, n_3, \dots, n_D), \quad (27)$$

$$\mathbf{y}_{\mathbf{n}}^+ = 2\mathbf{L}_{\mathbf{n}} + \mathbf{y}, \quad (28)$$

$$\mathbf{y}_{\mathbf{n}}^- = 2\mathbf{L}_{\mathbf{n}} - \mathbf{y}, \quad (29)$$

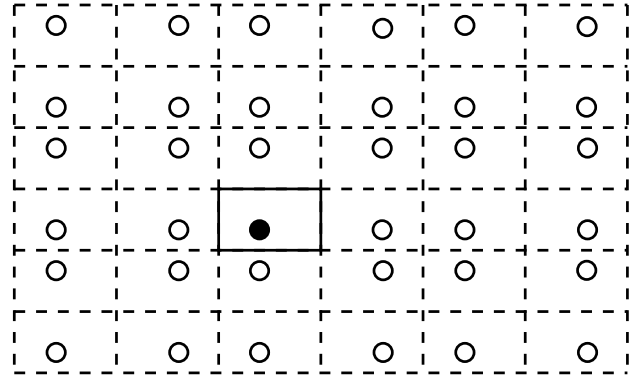
$$\mathbf{L}_{\mathbf{n}} = (n_1 L_1, n_2 L_2, n_3 L_3, \dots, n_D L_D), \quad (30)$$

where the sum (now a  $D$ -fold sum) runs over all possible combinations of the index vector  $\mathbf{n}$ . Note that a generalization has been included, in that the space dimension  $D_s$  of the monopole transfer function  $\mathcal{M}_{D_s}(r, \omega)$ , is not necessarily the same as the space dimension of the room  $D$ . The formulation allows any kind of relationship between  $D_s$ , and  $D$ ;  $D_s$  can be smaller, greater, or equal to  $D$ . In our physical space, and for radial sound fields with no angular dependence, these are restricted to  $(D, D_s) \leq 3$ , but still, both can be related in any way within this restriction. Figure 2 shows the distribution of image sources in  $D = 1$ . Figure 3 shows the distribution of image sources in  $D = 2$ . In these illustrated cases, with the listener in line, or in plane with the image sources, the room geometry has dimensions  $D = 1, 2$ , as implied by the distribution of image sources. However, the source transfer functions adopt the dimension of the embedding space:  $D_s = 3$ .

## 4. IMPLEMENTATION AND RESULTS

Implementation involves the following procedures:

- Define the room geometry (dimension  $D$ , etc.), wall reflection coefficients, sound source location, and listening location. Optionally, a different dimension  $D_s$  for the source transfer function.


 Figure 3. Distribution of image sources in  $D = 2$ .

- Generate the impulse response using the method of image sources, Eq. 24, up to a certain order.
- For each image source, take into account the time delay:  $r/c_0$ , attenuation with distance:  $1/r^{(D_s-1)/2}$ , and wall absorption, but do not implement at this stage the frequency weighting implied by the time derivatives. See Eqs. 10, 11, 12, Section 2.1.
- Take an audio signal, preferably a dry anechoic recording, and implement a fast convolution with the room's impulse response. This time, also apply the frequency weighting:  $(j\omega)^{(D_s-1)/2}$ .

Deferring the frequency weighting to a later stage in the processing, allows the option of removing, or changing it, preserving the image source calculation.

Impulses responses were generated coding in C and GNU Octave, using the parameters of one of the rooms simulated in  $D = 3$ , with  $f_s = 8$  kHz, and 37,500 image sources (up to about order  $n = \pm 16$ ), by Allen and Berkley [8]:

$$\mathbf{L} = (3.43, 5.15, 4.29), \quad (31)$$

$$\mathbf{x} = (2.14, 0.43, 2.57), \quad (32)$$

$$\mathbf{y} = (1.29, 4.29, 1.72), \quad (33)$$

$$\mathbf{R}_0 = (0.70, 0.90, 0.90), \quad (34)$$

$$\mathbf{R}_L = (0.70, 0.90, 0.90), \quad (35)$$

with longitudinal units in meters (after the originals reported in sampling periods), and sets of reflection coefficients:  $\mathbf{R}_0, \mathbf{R}_L$ , whose components  $n$  are the reflection coefficients of the walls defined by  $x_n = 0$ , and  $x_n = L_n$ , respectively. Rooms of dimensions  $D = 1$  to 6 were defined using these parameters, by including the first ( $D = 1$ ), then successive ( $D = 2, 3$ ), then recycling ( $D = 4, 5, 6$ ) components from the data set. Sampling frequency was the same,  $f_s = 8$  kHz, and image sources were calculated to order  $n = \pm 64$ , which for  $D = 3$ , add up to  $N = 129^3 = 2,146,689$  image sources. Figure 4 shows impulse responses in rooms of space dimensions  $D = 1$  to 6,  $D_s = D$ . Figure 5 shows impulse responses with monopole transfer functions of fixed dimension:  $D_s = 3$ . Both figures include frequency weightings:  $(j\omega)^{(D_s-1)/2}$ . Figure 6 shows the calculation times.

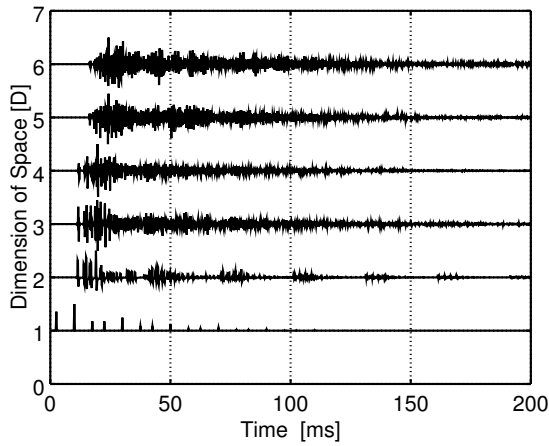


Figure 4. Impulse responses in rooms of space dimensions  $D = 1$  to  $6$ ,  $D_s = D$ , including:  $(j\omega)^{(D_s-1)/2}$ . Absolute peak amplitudes are normalized to 0.5 vertical units.

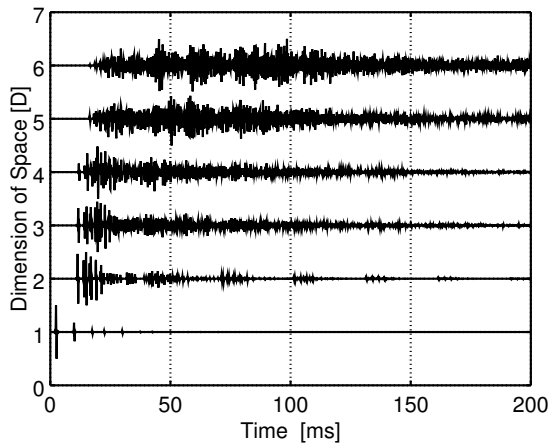


Figure 5. Impulse responses for source transfer functions of fixed dimension:  $D_s = 3$ , including:  $(j\omega)^{(D_s-1)/2}$ .

## 5. DISCUSSION

From a graphical analysis of the impulse responses, and also from the perceptual experience of listening to audio processed through them, it is possible to conclude that with increasing dimension  $D$ , there is increased and more intricate reverberation, with a consequently reduced intelligibility, and even with strong *aftermaths* at the higher dimensions. These are caused by the lumping together of reflections that get mapped into the same neighboring sampling periods (also perceptually) in certain portions of the impulse response. At the lower dimensions (especially  $D = 1, 2$ ), there are more chances of *flutter* and *pulsation* effects, while at the higher dimensions, sound tends to increasingly acquire *hissing* and *chirping* effects.

When using a source transfer function of fixed dimension, Figure 5, reverberation effects are noticeably reduced for rooms with  $D < D_s$ , but are over-emphasized when  $D > D_s$ . This occurs because, compared to the normal radial decay  $1/r^{(D-1)/2}$ , the radial decay  $1/r^{(D_s-1)/2}$  has little reach for  $D < D_s$ , but is more far reaching for  $D > D_s$ .

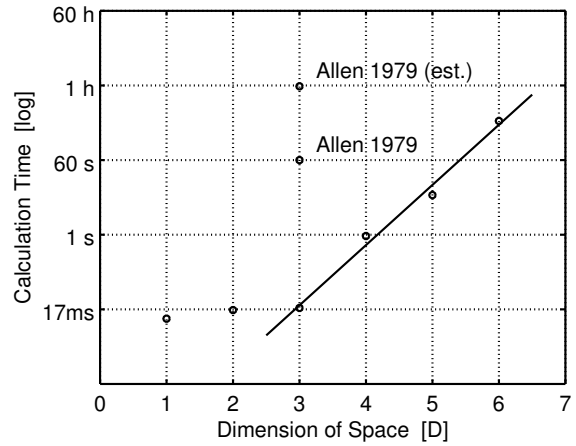


Figure 6. Calculation times for the generation of impulse responses in rooms of dimensions  $D = 1$  to  $6$ . Timings of Allen 1979 for  $N = 37,500$  image sources [8], and also estimated (est.) for  $N = 2, 146, 689$ , used here for  $D = 3$ .

## 6. CONCLUSIONS

Auralization procedures have been presented to produce sound signals that correspond to the analogue of acoustic propagation in free field, and room reverberation, in spaces of arbitrary higher dimensions  $D$ . Processing as presented here is monaural, but the mathematical tools exist to imprint a hyper-angular dependence in higher dimensions, and to map that into conventional binaural presentations. Applications are foreseen in the fields of sonic art, virtual reality, extended reality, videogames, computer games, etc.

## 7. REFERENCES

- [1] S.-H. Dong, *Wave Equations in Higher Dimensions*. Springer-Verlag, 2011.
- [2] J. Avery, *Hyperspherical Harmonics: Applications in Quantum Theory*. Springer-Verlag, 1989.
- [3] S. M. Al-Jaber, "Hydrogen Atom in  $N$  Dimensions," *International Journal of Theoretical Physics*, vol. 37, no. 4, pp. 1289–1298, 1998.
- [4] H. Hosoya, "Back-of-Envelope Derivation of the Analytical Formulas of the Atomic Wave Functions of a  $D$ -Dimensional Atom," *International Journal of Quantum Chemistry*, vol. 64, pp. 35–42, 1997.
- [5] G. Dassios and A. Fokas, "Methods for solving elliptic PDE's in spherical coordinates," *SIAM J. Appl. Math.*, vol. 68, no. 4, pp. 1080–1096, 2008.
- [6] R. L. Liboff, "Complex Hyperspherical Equations, Nodal-Partitioning, and First-Excited-State Theorems in  $\mathbb{R}^n$ ," *International Journal of Theoretical Physics*, vol. 41, no. 10, pp. 1957–1970, October 2001.
- [7] W.-Q. Zhao, "Relation Between Dimensional and Angular Momentum for Radially Symmetric Potential in  $N$ -Dimensional Space," *Commun. Theor. Phys.*, vol. 46, no. 3, pp. 429–434, September 2006.
- [8] J. B. Allen and D. A. Berkley, "Image method for efficiently simulating small-room acoustics," *Journal of the Acoustical Society of America*, vol. 65, no. 4, pp. 943–950, April 1979.
- [9] J. S. Avery, "Harmonic polynomials, hyperspherical harmonics, and atomic spectra," *Journal of Computational and Applied Mathematics*, vol. 233, pp. 1366–1379, 2010.
- [10] T. Kereselidze, G. Ckdua, P. Defrance, and J. Ogilvie, "Derivations, properties and applications of Coulomb Sturmians defined in spheroidal coordinates," *Molecular Physics*, vol. 114, no. 1, pp. 148–161, 2016.
- [11] Antti Kelloniemi and Vesa Välimäki and Patty Huang and Lauri Savioja, "Artificial reverberation using a hyper-dimensional FDTD mesh," in *13th European Signal Processing Conference*, IEEE Conference Publications, Ed., 2005, pp. 1–4.
- [12] Antti Kelloniemi and Patty Huang and Vesa Välimäki and Lauri Savioja, "Hyper-Dimensional Digital Waveguide Mesh for Reverberation Modeling," in *CiteSeerX* <https://core.ac.uk/doi/10.1.1.384.708.2013-12-08>, 2013.